Multicolor Barcoding in a Single Upconversion Crystal

Yuhai Zhang,[†] Lixin Zhang,[‡] Renren Deng,[†] Jing Tian,[§] Yun Zong,[∥] Dayong Jin,[‡] and Xiaogang Liu*,[†,∥,⊥]

[†]Department of Chemistry, National University of Singapore, 3 Science Drive 3, Singapore 117543, Singapore

[‡]Advanced Cytometry Laboratories, MQ Photonics Research Centre and MQ Biofocus Research Centre, Macquarie University, Sydney, NSW 2109, Australia

[§]Laboratory of Advanced Materials, Fudan University, 220 Handan Road, Shanghai 200433, China

[∥]Institute of Materials Research and Engineering, 3 Research Link, Singapore 117602, Singapore
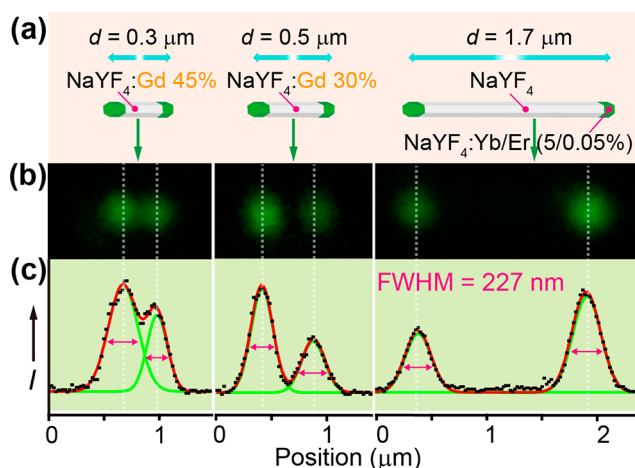
[⊥]Center for Functional Materials, NUS (Suzhou) Research Institute, Suzhou, Jiangsu 215123, China

S *Supporting Information*

ABSTRACT: We report the synthesis of luminescent crystals based on hexagonal-phase $NaYF_4$ upconversion microrods. The synthetic procedure involves an epitaxial end-on growth of upconversion nanocrystals comprising different lanthanide activators onto the $NaYF_4$ microrods. This bottom-up method readily affords multicolor-banded crystals in gram quantity by varying the composition of the activators. Importantly, the end-on growth method using one-dimensional microrods as the template enables facile multicolor tuning in a single crystal, which is inaccessible in conventional upconversion nanoparticles. We demonstrate that these novel materials offer opportunities as optical barcodes for anticounterfeiting and multiplexed labeling applications.

Figure 1. (a) Schematic design for determining the diffraction limit of the microscope using three tip-modified microrods with different spacer lengths (d = 0.3, 0.5, and 1.7 μm). (b) Upconversion micrographs of the three microrods showing the emission dots from the tips. (c) Their corresponding emission spectra indicating the degree of the spatial overlap between the two emission dots. The point spread function (red line) of the intensity profile is fitted with a Gaussian function (green line), and the full width at half-maximum (fwhm) is taken as the resolution. The average fwhm of the six spots is 227 nm, in good agreement with the theoretical value (196 at 550 nm estimated using an oil objective lens with a numeric aperture of 1.4). Note that the length of the spacer is tuned by Gd doping at varied concentrations.

B arcoding materials have been widely used as luminescent probes for multiplexed assays in biological species because of their distinct optical characteristics.[1] The use of these materials for anticounterfeiting applications has also attracted much attention in recent years.[2] However, their application in practical settings has been largely hindered by high-cost materials fabrication, low reaction yields, complex instrumentation setup, and high background noise when excited by common ultraviolet or visible light sources.[3]

Lanthanide-doped upconversion materials may provide a much needed solution for the above-mentioned problems.[4] First, their fabrication methods are typically based on low-cost bottom-up processes and can be easily scaled up for massive production.[5] Second, the morphology of the upconversion materials is highly tunable with features ranging from nanosized particles to microscale rods,[6] allowing for direct decoding without the concern of the diffraction limit using conventional optical microscopes. The third aspect is that upconversion materials feature large anti-Stokes shifts and long lifetimes, leading to largely reduced background noise.[7] Furthermore, the ability to tune the emission wavelength from UV–vis to NIR spectral regions offered by photon upconversion enables the generation of a large, diverse library of optical barcodes. Despite their promise, it has been challenging to prepare multicolored upconversion barcodes using a single spherical nanoparticle due to the resolution limit of conventional optical microscopes. Herein, we report the rational design and synthesis of multicolor-banded upconversion barcodes based on tip-modified hexagonal-phase $NaYF_4$ microrods with different activators doped at the tips (Scheme 1). With varying sets of activators, we prepare a library of single-crystal-based upconversion barcodes comprising different combinations of three primary colors (red, green, and blue) that are easily readable with conventional optical microscopes. We also demonstrate the use of these optical materials as barcodes for security inking and cell tracking applications.

Regular light microscopes generally have the best spatial resolution of ~200 nm constrained by the optical diffraction limit.[8] To resolve two emission features (or spots), the two
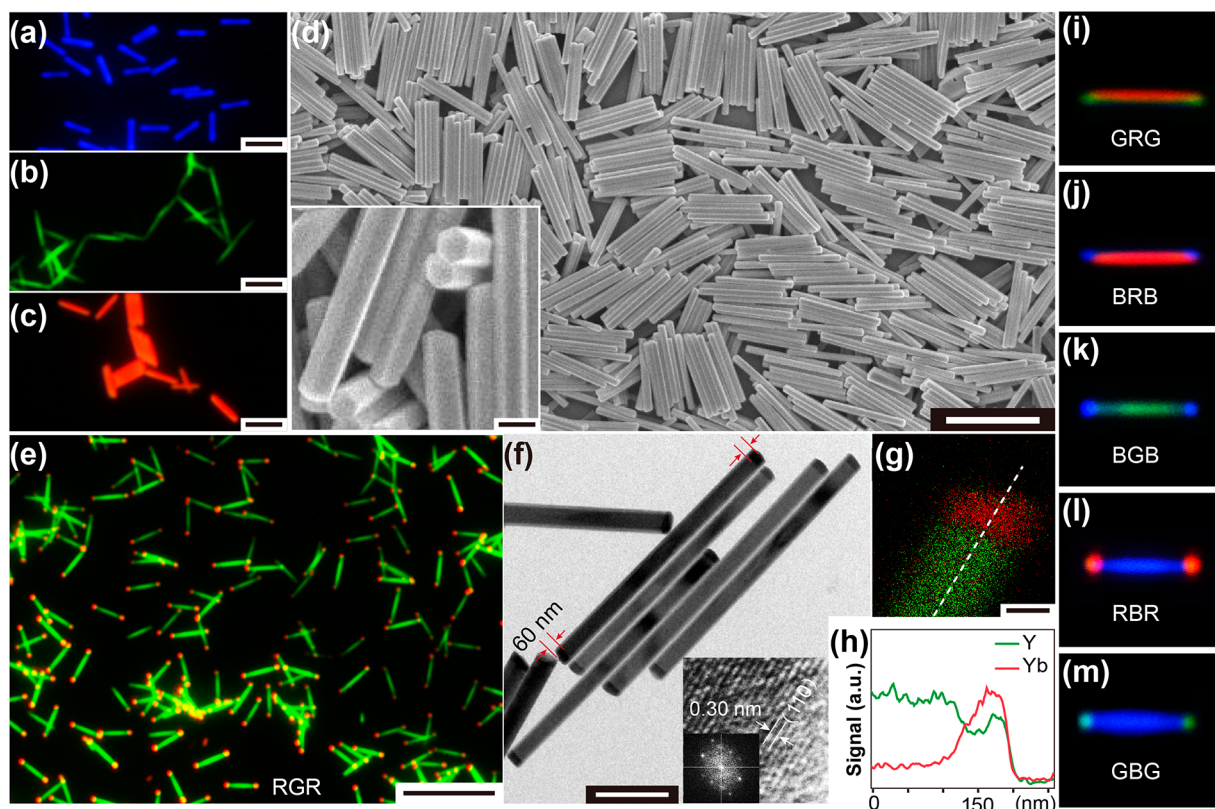
Figure 2. (a−c) Optical micrographs of the parent $NaYF_4$ upconversion microrods doped with Yb^{3+}/Tm^{3+} (20/0.2 mol %), Yb^{3+}/Er^{3+} (5/0.05 mol %), and Yb^{3+}/Er^{3+} (50/0.05 mol %), respectively. Scale bars in a-c are 2 μm. (d) A typical SEM image of the $NaYF_4$ microrods. Scale bar is 2 μm. Inset shows the hexagonal prism morphology of the rods. Scale bar is 200 nm. (e) Optical micrographs of dual-color (RGR) emitting $NaYF_4$ microrods after the end-on epitaxial growth with $NaYF_4$:Yb/Er precursors. Scale bar is 5 μm. Note that the red-emitting tips are heavily doped with 50 mol % of Yb^{3+}, while the green-emitting segment is doped with 5 mol % of Yb^{3+}. (f) TEM image of the tip-modified microrods (Inset: HRTEM image and corresponding Fourier-transform diffractogram of the segment joint). Scale bar is 500 nm. (g, h) Elemental mapping and corresponding EELS line scan conducted on a single tip-modified microrod. Scale bar in g is 50 nm. (i−m) Optical micrographs showing five additional sets of dual-color-banded upconversion microrods, obtained by varying the composition of the dopants. Note that the appearance of a tinge color at the tip junction is due to the chromatic aberration and limited resolution of the microscope.

emitting objects need to be separated by a distance larger than the diffraction limit. Otherwise, the microscope would not have the necessary resolution power to distinguish them. In our design, we utilize $NaYF_4$ microrods with a length of ~2 μm as spacers to grow tip-modified rods that can exhibit distinguishable dual-color emissions. To confirm this, we synthesized three types of microrods with emitting tips separated by spacers of different lengths (Figures 1 and S1). It was found that as the length of the spacer increases from 0.3 to 1.7 μm, the two emitting spots are gradually resolved from one merged spot into two independent spots. Considering the compromise of synthetic yield induced by Gd^{3+} doping (detailed discussion in Supporting Information),[6a] we chose a 1.7-μm spacer in this work for multicolor tuning on a single upconversion crystal. The use of the 1.7-μm spacer for the growth of tip-modified rods overcomes the diffraction limit, allowing different emission colors easily resolvable at the single crystal level.

The lanthanide-doped $NaYF_4$ microrods were prepared by a well-established hydrothermal method.[9] Emissions from individual rods doped with different sets of lanthanides can be identified owing to the strong upconversion luminescence of the hexagonal-phase microrods (Figures 2a−c and S2). Scanning electron microscopic imaging reveals the high uniformity of the as-synthesized microrods (~1.9 μm in length and ~140 nm in diameter) (Figure 2d). Note that the length of the rods can

be tuned from 0.3 to 2 μm using the gadolinium doping approach (Figure S1).[10] Furthermore, we found that upon addition of α-$NaYF_4$ nanoparticles (Figure S3) as the precursors, successive end-on growth of the β-$NaYF_4$ microrods can be achieved, as evidenced by the optical microscopic images (Figure 2e). This can be attributed to favorable epitaxial growth along the long [001] axis of the crystal. Transmission electron microscopy (TEM) imaging shows two dark-colored tips of the segmented rods, attributable to the high contrast of heavily Yb^{3+}-doped $NaYF_4$ (Figures 2f and S12). High-resolution TEM reveals the single-crystalline nature of the rod with a d-spacing of 0.30 nm, corresponding to the (110) plane of β-$NaYF_4$ (JCPDS No. 16-0334). X-ray diffraction data suggest that the α-$NaYF_4$ precursors are completely consumed after the hydrothermal reaction (Figure S4).

To confirm the tip growth onto the parent microrod, we intentionally doped Yb^{3+} with large concentration disparities, into the β-$NaYF_4$:Yb/Er microrod (5 mol % of Yb^{3+}) and the α-$NaYF_4$:Yb/Er nanoparticle precursor (50 mol % of Yb^{3+}), respectively (Figure S4). Elemental mapping by STEM was performed on the resulting hybrid rods. The difference in the elemental distribution of Yb^{3+} and Y^{3+} over the rod tip clearly indicates the presence of a junction (Figure 2g). The line scan and spot scan analyses reveal the Yb abundance (40%) in the new tip, which is in good agreement with the Yb content in

Scheme 1. Design of the Bottom-up Synthesis of a Dual-Color-Banded Hexagonal-Phase NaYF$_4$:Yb/Er Upconversion Microrod through an Oriented Epitaxial Growth Method[a]
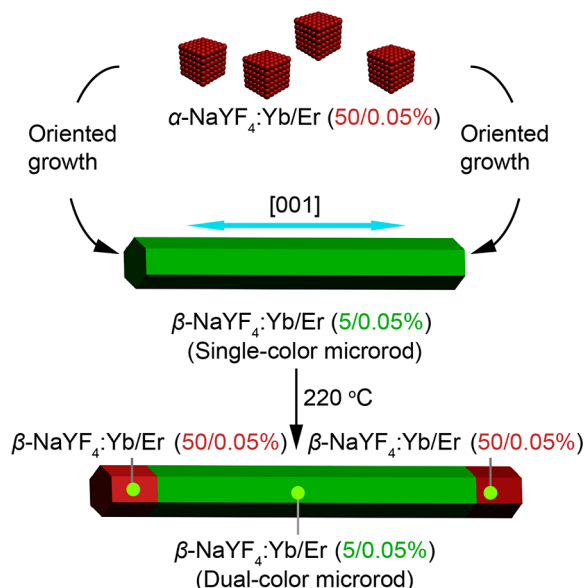
[a]As cubic-phase NaYF$_4$ nanoparticles tend to dissolve at elevated temperatures due to low thermal stability, they could be used as precursors for successive growth of hexagonal-phase NaYF$_4$ tips at both ends of the microrods.
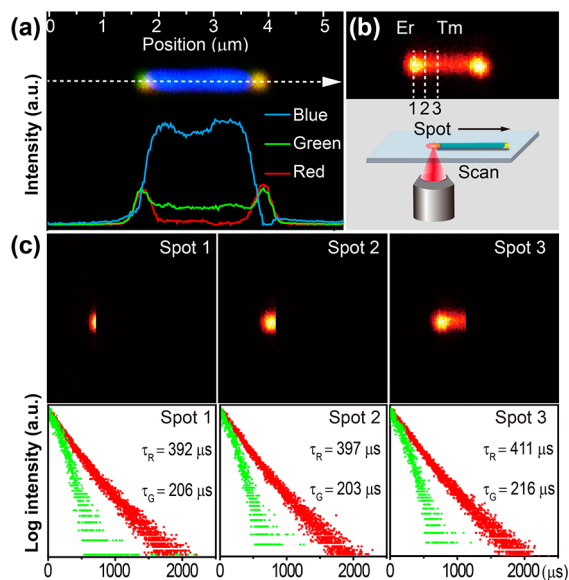
Figure 3. (a) Wide-field luminescence image of a single microrod exhibiting YBY dual-color upconversion emission. Note that the color component of the emission can be resolved by RGB acquisition. (b) Confocal microscope image of a different dual-color microrod. (c) The corresponding green ($^4S_{3/2}$) and red ($^4F_{9/2}$) emission lifetimes in three different areas (marked with spot 1, 2, 3 shown in b) of the microrod. Note that spot 1 contains only Er^{3+}. Spot 2 contains Er^{3+} and a small amount of Tm^{3+}. Spot 3 is codoped with Er^{3+} and a large amount of Tm^{3+}.

α-NaYF$_4$ precursors (Figures 1h and S5). Importantly, the use of α-NaYF$_4$ nanoparticle precursors rather than lanthanide ionic solutions is critical for high yield synthesis of the segmented microrods, as the direct use of ionic precursors leads to phase separation dominant in the crystal growth process
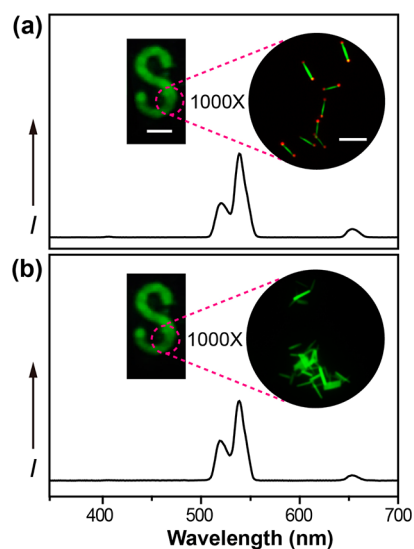
Figure 4. (a) Luminescence image of a stamped letter S generated with dual-color microrods (shown in 1000× magnified image) as the ink. The corresponding upconversion emission spectrum is also shown. Scale bars are 3 μm (right) and 3 mm (left). (b) Luminescence image of a control sample generated with single-color microrods as the ink. Note that the emission spectra (or bulk color appearance) of these two patterns are almost identical. However, their differences in spatial distribution are clearly distinguishable under high magnification.

(Figure S6).[11] It is worth noting that the introduction of luminescent tips of different composition not only enhances the color contrast of the parent microrod but also expands the scope of multicolor upconversion at the single crystal level. Using the step-by-step epitaxial growth method, we synthesized a series of dual-color upconversion microrods displaying different combinations of three primary colors (Figure 2i–m).

As an added benefit, the dual-color upconversion microrod provides a platform to investigate the possibility of energy transfer at the tip junction. To this end, we synthesized YBY-color rods (Y and B denote yellow emission of the tips and blue emission of the parent rod, respectively) (Figure 3a). Using a confocal microscope (Figure S7), three different spots (Labeled as 1, 2, 3) at the region of the tip junction can be selectively focused and scanned (Figure 3b). Notably, the use of different band-pass filters allows us to analyze the individual emission peak of Er^{3+}, for example, green emission at 545 nm ($^4S_{3/2} \rightarrow$ $^4I_{15/2}$) and red peak at 655 nm ($^4F_{9/2} \rightarrow$ $^4I_{15/2}$) (Figure S8). We obtained essentially unaltered lifetimes of Er^{3+} recorded at three different spots (Figures 3c and S9), indicating that there is no crosstalk between Tm^{3+} and Er^{3+} activators even at the tip junction. We reason that the intrinsic small absorption cross sections ($\sim10^{-21}$ cm^2) of lanthanide ions and the relatively large donor−acceptor separation at the tip junction are mainly responsible for the inefficient energy transfer between Tm^{3+} and Er^{3+}.[12]

We further demonstrated the use of the as-synthesized multicolor microrods as barcodes for anticounterfeiting application.[13] Note that these microrods are dispersible in dimethyl sulfoxide solvent, providing a transparent ink solution under ambient light conditions (Figure S10). As a proof-of-concept experiment, we stamped a solution containing RGR dual-color emitting NaYF$_4$:Yb/Er microrods (Yb^{3+}/Er^{3+}: 5/0.05 mol % for the green-emitting part and Yb^{3+}/Er^{3+}: 50/0.05 mol % for the red-emitting ends) as the security ink onto a paper substrate to

create an "S" pattern. As a control, we generated an identical pattern using green-color emitting NaYF$_4$:Yb/Er (10/0.05 mol %) microrods. When exposed to 980-nm laser light, the two patterns are almost indistinguishable based on emission spectral comparison or color appearance under low magnification (Figure 4a). Remarkably, we could clearly tell the two patterns apart when zoomed in under high magnification (Figure 4b). These experiments revealed that the dual-color spatially coded microrods can provide added security protection, enabling almost instant verification of patterned features. On a separate note, these microrods can be internalized by cancer cells, posing positive implications in the quest for multiplexed optical labels (Figure S11 and Movie S1).

Our findings could bring a better understanding of epitaxial growth to other lanthanide-based anisotropic crystals. The fact that these solution-processable multicolor-banded microrods with good crystalline properties can be easily made on a large scale suggests the prospects of using upconversion phosphor barcodes for optical labeling applications, where low-cost manufacturing of the materials with multilevel optical features is essential. We expect an increased effort dedicated to the investigation of these materials in the near future.

■ ASSOCIATED CONTENT

ⓢ Supporting Information

Additional experimental details. This material is available free of charge via the Internet at http://pubs.acs.org.

■ AUTHOR INFORMATION

Corresponding Author
chmlx@nus.edu.sg

Notes
The authors declare no competing financial interest.

■ ACKNOWLEDGMENTS

■ REFERENCES

(1) (a) Nam, J.-M.; Thaxton, C. S.; Mirkin, C. A. *Science* **2003**, *301*, 1884. (b) Agasti, S. S.; Liong, M.; Peterson, V. M.; Lee, H.; Weissleder, R. *J. Am. Chem. Soc.* **2012**, *134*, 18499. (c) Kim, S. H.; Shim, J. W.; Yang, S. M. *Angew. Chem., Int. Ed.* **2011**, *50*, 1171. (d) Pregibon, D. C.; Toner, M.; Doyle, P. S. *Science* **2007**, *315*, 1393.

(2) (a) Osberg, K. D.; Rycenga, M.; Bourret, G. R.; Brown, K. A.; Mirkin, C. A. *Adv. Mater.* **2012**, *24*, 6065. (b) Creran, B.; Yan, B.; Moyano, D. F.; Gilbert, M. M.; Vachet, R. W.; Rotello, V. M. *Chem. Commun.* **2012**, *48*, 4543.

(3) (a) Haase, M.; Schäfer, H. *Angew. Chem., Int. Ed.* **2011**, *50*, 5808. (b) Gorris, H. H.; Wolfbeis, O. S. *Angew. Chem., Int. Ed.* **2013**, *52*, 3584. (c) Park, Y. I.; Nam, S. H.; Kim, J. H.; Bae, Y. M.; Yoo, B.; Kim, H. M.; Jeon, K.; Park, H. S.; Choi, J. S.; Lee, K. T.; Suh, Y. D.; Hyeon, T. *J. Phys. Chem. C* **2013**, *117*, 2239. (d) Bogdan, N.; Vetrone, F.; Ozin, G. A.; Capobianco, J. A. *Nano Lett.* **2011**, *11*, 835. (e) Chen, G.; Ohulchanskyy, T. Y.; Liu, S.; Law, W.; Wu, F.; Swihart, M. T.; Agren, H.; Prasad, P. N. *ACS Nano* **2012**, *6*, 2969. (f) Hao, J.; Zhang, Y.; Wei, X. *Angew. Chem., Int. Ed.* **2011**, *50*, 6876. (g) Li, L.; Wu, P.; Hwang, K.; Lu, Y. *J. Am. Chem. Soc.* **2013**, *135*, 2411. (h) Zhou, J.; Liu, Z.; Li, F. *Chem. Soc. Rev.* **2012**, *41*, 1323. (i) Liu, Y.; Zhou, S.; Tu, D.; Chen, Z.; Huang, M.; Zhu, H.; Ma, E.; Chen, X. *J. Am. Chem. Soc.* **2012**, *134*, 15083.

(4) (a) Zhang, F.; Haushalter, R. C.; Haushalter, R. W.; Shi, Y.; Zhang, Y.; Ding, K.; Zhao, D.; Stucky, G. D. *Small* **2011**, *7*, 1972. (b) Podhorodecki, A.; Banski, M.; Noculak, A.; Sojka, B.; Pawlik, G.; Misiewicz, J. *Nanoscale* **2013**, *5*, 429. (c) Wang, F.; Deng, R.; Wang, J.; Wang, Q.; Han, Y.; Zhu, H.; Chen, X.; Liu, X. *Nat. Mater.* **2011**, *10*, 968. (d) Hu, W.; Lu, X.; Jiang, R.; Fan, Q.; Zhao, H.; Deng, W.; Zhang, L.; Huang, L.; Huang, W. *Chem. Commun.* **2013**, *49*, 9012. (e) Teng, X.; Zhu, Y.; Wei, W.; Wang, S.; Huang, J.; Naccache, R.; Hu, W.; Tok, A. I. Y.; Han, Y.; Zhang, Q.; Fan, Q.; Huang, W.; Capobianco, J. A.; Huang, L. *J. Am. Chem. Soc.* **2012**, *134*, 8340. (f) Saboktakin, M.; Ye, X.; Chettiar, U. K.; Engheta, N.; Murray, C. B.; Kagan, C. R. *ACS Nano* **2013**, *7*, 7186. (g) Chan, E. M.; Han, G.; Goldberg, J. D.; Gargas, D. J.; Ostrowski, A. D.; Schuck, P. J.; Cohen, B. E.; Milliron, D. J. *Nano Lett.* **2012**, *12*, 3839. (h) Schäfer, H.; Ptacek, P.; Eickmeier, H.; Haase, M. *Adv. Funct. Mater.* **2009**, *19*, 3091. (i) Ye, X.; Collins, J. E.; Kang, Y.; Chen, J.; Chen, D. T. N.; Yodh, A. G.; Murray, C. B. *Proc. Natl. Acad. Sci. U.S.A.* **2010**, *107*, 22430. (j) Liu, Y.; Tu, D.; Zhu, H.; Chen, X. *Chem. Soc. Rev.* **2013**, *42*, 6924.

(5) (a) Dai, Y.; Xiao, H.; Liu, J.; Yuan, Q.; Ma, P. a.; Yang, D.; Li, C.; Cheng, Z.; Hou, Z.; Yang, P.; Lin, J. *J. Am. Chem. Soc.* **2013**, *135*, 18920. (b) Liu, Q.; Sun, Y.; Yang, T.; Feng, W.; Li, C.; Li, F. *J. Am. Chem. Soc.* **2011**, *133*, 17122. (c) Anderson, R. B.; Smith, S.; May, P. S.; Berry, M. T. *J. Phys. Chem. Lett.* **2014**, *5*, 36.

(6) (a) Wang, F.; Han, Y.; Lim, C. S.; Lu, Y.; Wang, J.; Xu, J.; Chen, H.; Zhang, C.; Hong, M.; Liu, X. *Nature* **2010**, *463*, 1061. (b) Wang, L.; Li, Y. *Nano Lett.* **2006**, *6*, 1645. (c) Zhang, F.; Wan, Y.; Yu, T.; Zhang, F.; Shi, Y.; Xie, S.; Li, Y.; Xu, L.; Tu, B.; Zhao, D. *Angew. Chem., Int. Ed.* **2007**, *46*, 7976. (d) Zhang, C.; Lee, J. Y. *ACS Nano* **2013**, *7*, 4393. (e) Na, H.; Woo, K.; Lim, K.; Jang, H. S. *Nanoscale* **2013**, *5*, 4242. (f) Xiao, Q.; Zheng, X.; Bu, W.; Ge, W.; Zhang, S.; Chen, F.; Xing, H.; Ren, Q.; Fan, W.; Zhao, K.; Hua, Y.; Shi, J. *J. Am. Chem. Soc.* **2013**, *135*, 13041. (g) Zhou, J.; Chen, G.; Wu, E.; Bi, G.; Wu, B.; Teng, Y.; Zhou, S.; Qiu, J. *Nano Lett.* **2013**, *13*, 2241. (h) Stanton, I.; Ayres, J. A.; Therien, M. J. *Dalton Trans.* **2012**, *41*, 11576.

(7) (a) Auzel, F. *Chem. Rev.* **2004**, *104*, 139. (b) Beurer, E.; Grimm, J.; Gerner, P.; Güdel, H. U. *J. Am. Chem. Soc.* **2006**, *128*, 3110. (c) Eliseeva, S. V.; Bünzli, J.-C. G. *Chem. Soc. Rev.* **2010**, *39*, 189. (d) Wang, F.; Liu, X. *Chem. Soc. Rev.* **2009**, *38*, 976.

(8) (a) Caillat, L.; Hajj, B.; Shynkar, V.; Michely, L.; Chauvat, D.; Zyss, J.; Pellé, F. *Appl. Phys. Lett.* **2013**, *102*, 143114. (b) Cui, J.-M.; Sun, F.-W.; Chen, X.-D.; Gong, Z.-J.; Guo, G.-C. *Phys. Rev. Lett.* **2013**, *110*, 153901.

(9) Wang, X.; Zhuang, J.; Peng, Q.; Li, Y. *Nature* **2005**, *437*, 121.

(10) (a) Chen, D.; Yu, Y.; Huang, F.; Yang, A.; Wang, Y. *J. Mater. Chem.* **2011**, *21*, 6186. (b) Zeng, S.; Ren, G.; Xu, C.; Yang, Q. *CrystEngComm* **2011**, *13*, 4276.

(11) (a) Johnson, N. J.; Korinek, A.; Dong, C.; van Veggel, F. C. *J. Am. Chem. Soc.* **2012**, *134*, 11068. (b) Li, C.; Yang, J.; Quan, Z.; Yang, P.; Kong, D.; Lin, J. *Chem. Mater.* **2007**, *19*, 4933.

(12) (a) Su, Q.; Han, S.; Xie, X.; Zhu, H.; Chen, H.; Chen, C.-K.; Liu, R.-S.; Chen, X.; Wang, F.; Liu, X. *J. Am. Chem. Soc.* **2012**, *134*, 20849. (b) Wang, J.; Deng, R.; MacDonald, M. A.; Chen, B.; Yuan, J.; Wang, F.; Chi, D.; Hor, T. S. A.; Zhang, P.; Liu, G.; Han, Y.; Liu, X. *Nat. Mater.* **2014**, *13*, 157. (c) Xie, X.; Liu, X. *Nat. Mater.* **2012**, *11*, 842. (d) Xie, X.; Gao, N.; Deng, R.; Sun, Q.; Xu, Q.-H.; Liu, X. *J. Am. Chem. Soc.* **2013**, *135*, 12608.

(13) (a) Lu, Y.; Zhao, J.; Zhang, R.; Liu, Y.; Liu, D.; Goldys, E. M.; Yang, X.; Xi, P.; Sunna, A.; Lu, J.; Yu, Shi.; Robert, C. L.; Huo, Y.; Shen, J.; Piper, J. A.; Robinson, J. P.; Jin, D. *Nat. Photonics* **2013**, *8*, 32. (b) Deng, R.; Liu, X. *Nat. Photonics* **2014**, *8*, 10. (c) Zhao, J.; Jin, D.; Schartner, E. P.; Lu, Y.; Liu, Y.; Zvyagin, A. V.; Zhang, L.; Dawes, J. M.; Xi, P.; Piper, J. A.; Goldys, E. M.; Monro, T. M. *Nat. Nanotechnol.* **2013**, *8*, 729. (d) Zhang, Y.; Liu, X. *Nat. Nanotechnol.* **2013**, *8*, 702. (e) Liu, Y.; Ai, K.; Lu, L. *Nanoscale* **2011**, *3*, 4804. (f) Meruga, J. M.; Cross, W. M.; May, P. S.; Luu, Q.; Crawford, G. A.; Kellar, J. J. *Nanotechnology* **2012**, *23*, 395201. (g) Wang, J.; Wei, T.; Li, X.; Zhang, B.; Wang, J.; Huang, C.; Yuan, Q. *Angew. Chem., Int. Ed.* **2014**, *53*, 1616.